Nonlocal coupling can prevent the collapse of spatiotemporal chaos

Safia Yonker and Renate Wackerbauer*
Department of Physics, University of Alaska, Fairbanks, Alaska 99775-5920, USA
(Received 15 September 2005; published 23 February 2006)

Spatiotemporal chaos on a regular ring network of excitable Gray-Scott dynamical elements is transient. We find that the addition of very few nonlocal network connections drastically changes the average lifetime of spatiotemporal chaos. In the presence of a single shortcut local interface formation delays the collapse of spatiotemporal chaos. This competes with a reduced average characteristic path length that advances the collapse process. Two added shortcuts can prevent the collapse of spatiotemporal chaos by causing an asymptotic local collapse.

DOI: 10.1103/PhysRevE.73.026218 PACS number(s): 05.45.Jn, 89.75.Hc

I. INTRODUCTION

Transient spatiotemporal chaos is a generic pattern in extended nonequilibrium systems across several disciplines. In the absence of external perturbations, the spatiotemporal complexity of the system changes spontaneously from chaotic to steady-state or periodic behavior. The mechanistic understanding of the collapse remains elusive, in contrast to low-dimensional systems where a chaotic repellor is known to govern transient chaos [1]. A collapse of spatiotemporal chaos has been reported in models for turbulent dynamics [2], for semiconductor charge transport [3], for CO oxidation on single-crystal Pt surfaces [4], for a cubic autocatalytic mass-action model [5], and in a system of coupled logistic maps [6]. In addition, spatiotemporal complexity with irregular dynamics and fast-decaying correlations but a negative maximum Lyapunov exponent ("stable chaos") was found to be transient in systems of coupled one-dimensional maps [7,8]. The collapse of spatiotemporal chaos has also been suggested as an explanation for species extinction in ecology [9,10].

The asymptotic stability of chaotic dynamics in extended systems is difficult to determine, since transient spatiotemporal chaos may be extremely long lived; its average lifetime typically increases exponentially with the size of the medium [3–5,8,11]. In realistic distributed systems noise and nonlocal coupling may influence the collapse process, which provides further difficulties in determining the asymptotic stability [12,13]. We study transient spatiotemporal chaos on ring networks with few added nonlocal couplings. The motivation stems from realistic biological, technological, and social network topologies that are neither completely regular nor completely random [14–18] and often have small-world [14] or scale-free properties [15].

It is commonly reported that network topology influences synchronization. Nonlocal coupling usually enhances synchronization behavior in networks [19–22], which is generally attributed to the smaller average path length in the network. In a heterogeneous distribution of connections, however, a well-connected and overloaded network node can prevent synchronization despite a reduced path length [23]; however, it can enhance synchronization if the coupling strength is weighted properly [24]. In all of these cases insight into the stability of the synchronized state in linearly coupled dynamical elements is given by the master stability function [20,25] and its generalization for weighted networks [26].

Nonlocal coupling induces various dynamical behavior in complex systems: Effects of scale-free networks include random walk behavior [27], coherence in coupled chaotic maps [28], vibrational modes in a Hamiltonian system of coupled harmonic oscillators [29], or the absence of epidemic thresholds [30]. Effects of small-world topologies include taming of asymptotic spatiotemporal chaos to spatially periodic motion at an optimum fraction of random shortcuts [31] and prolongation of chaotic transients by slightly reducing the degree of connectivity in a globally pulse-coupled random oscillator network [32]. In a coupled map lattice the second-order phase transition to turbulence via spatiotemporal intermittency became first order above some critical rewiring probability [33].

Nonlocal connections in a network also influence the dynamics of various excitable systems: Fast-response and coherent oscillations have been found in a neuronal layer [34]; self-sustained neural activity is caused by branching and reinjection of propagating activity pulses [35]; in an epidemiological model, the number of infected sites are oscillating with time at large rewiring probability [19]; spiral-wave propagation is sustained in the presence of small-world connections in a spatially inhomogeneous excitable medium [36].

In this paper we report that transient spatiotemporal chaos is clearly influenced by the addition of few nonlocal connections to a regular ring network of Gray-Scott excitable elements. We demonstrate in Sec. III that only a single shortcut can drastically change the lifetime of spatiotemporal chaos. Whether the lifetime is on average increased or decreased, however, depends on the length of the shortcut. In Sec. IV we discuss local dynamical consequences of the shortcut and how they influence the global dynamics to cause the change in the lifetime of spatiotemporal chaos. In Sec. V we show that two or more added shortcuts can make transient spatiotemporal chaos asymptotic.

*Electronic address: ffraw1@uaf.edu

II. THE MODEL

The network of N coupled, identical, continuous-time dynamical elements consists of an excitable system at each network node $n\,(n=1,2,\ldots,N)$ and diffusive coupling between the nodes.

The *excitable dynamics at each node* is given by the two-variable Gray-Scott model [37], which describes an open, autocatalytic reaction $A+2B\rightarrow 3B$ and $B\rightarrow C$, where A represents the reactant (resource), B the autocatalytic species, and C the final product. This reaction is modeled by the following coupled dimensionless differential equations:

$$\frac{da_n}{dt} = 1 - a_n - \mu a_n b_n^2 + \Delta_n(a_n),$$

$$\frac{db_n}{dt} = \mu a_n b_n^2 - \Phi b_n + \Delta_n(b_n). \tag{1}$$

where a_n and b_n are the dimensionless concentrations of resource A and species B at node n and Φ and μ are the bifurcation parameters, determined by the rate constants and the reactant concentration in the reservoir. The coupling term $\Delta_n(\cdot)$ depends on the connectivity of node n and the strength of the diffusive coupling.

The spatially uniform system is characterized by three steady states

$$S^n = (1,0),$$

$$S^f = \left(\frac{1-\sqrt{1-4\Phi^2/\mu}}{2}, \frac{1+\sqrt{1-4\Phi^2/\mu}}{2\Phi}\right),$$

$$S^s = \left(\frac{1+\sqrt{1-4\Phi^2/\mu}}{2}, \frac{1-\sqrt{1-4\Phi^2/\mu}}{2\Phi}\right).$$

Linear stability analysis shows that S^n is a stable node, which exists for all parameter values μ and Φ. S^f is an unstable focus and S^s is a saddle point, which exist for μ above the saddle node bifurcation, $\mu_{sn}=4\Phi^2$. In the range $2<\Phi<4$, S^f becomes a stable focus above the subcritical Hopf bifurcation point, $\mu_H=\Phi^4/(\Phi-1)$. In the parameter regime of interest $[\mu_{sn},\mu_H]$ and $\Phi=2.8$ the dynamical system at each node is excitable.

In a *regular ring network* the diffusive coupling is between next nearest neighbors and the boundary conditions are periodic. Resource concentration a and species concentration b follow the same Laplacian coupling scheme,

$$\Delta_n(x_n) = D([x_{n+1}-x_n]+[x_{n-1}-x_n]). \tag{2}$$

D determines the strength of the coupling, and each concentration gradient adds to the magnitude of nodal interaction.

On a regular ring network of Gray-Scott excitable elements [Eqs. (1) and (2)] the system dynamics exhibits transient spatiotemporal chaos [5]. After a regime of sustained spatiotemporal chaos with a rapid decay of spatial correlations [38,39] and a positive largest Lyapunov exponent [5], the system exhibits a spontaneous, intrinsic collapse to the homogeneous stable steady state S^n with extinct species. The spatiotemporally chaotic dynamics was characterized by a Šilnikov-type orbit that consists of a heteroclinic connection from the unstable focus S^f to the stable node S^n in the homogeneous system and a heteroclinic connection from S^n to S^f for the traveling wave system [38]. A typical trajectory at a network node spirals away from the unstable focus toward the stable node, only to be reinjected to the unstable focus via the propagating reaction-diffusion activity. The parameter range $[\mu_c,\mu_H]$ for wave-induced spatiotemporal chaos is determined by the critical threshold for traveling wave solutions μ_c and the Hopf bifurcation point μ_H, with $\mu_c\approx 33$ for $\Phi=2.8$ [38].

The regular ring topology in Eq. (2) is generalized to allow for *nonlocal coupling (shortcuts)* in the network. Each network node n is connected to its two neighrest neighbors and possibly to a third distant node $n+m$. Resource concentration a and species concentration b both follow the generalized Laplacian coupling scheme

$$\Delta_n(x_n,x_\kappa) = D_n \sum_{\kappa\in\mathbb{K}} (x_\kappa - x_n), \tag{3}$$

where $\mathbb{K}=\{n-1,n+1,n+m\delta_{3,k_n}\}$ and $|m|>1$. $\mathbb{K}$ represents the set of nodes connected to node n, and $k_n=2+\delta_{3,k_n}$ is the total number of connections to node n (excluding self-connections). The weighted coupling coefficient $D_n=2D/k_n$ depends on the uniform coupling parameter D from the regular network and on k_n [40]. For the case where node n is connected to only its two nearest neighbors, $D_n=D$ and Eq. (3) reduces to the expression for a regular network given in Eq. (2). The weighted coupling parameter D_n ensures that the perturbation Δ_n a node n is experiencing is the same on average for all nodes, independent of the number of connections made to it. It also ensures that any node n in a complex network, where k_n varies with n, experiences on average the same perturbation Δ_n as a node in the corresponding regular network, where $D_n=D$. Consequently differences in the dynamics on various networks of size N are due to differences in their topology, and not due to differences in perturbations Δ_n that might be caused by a well connected node. Weighing of the incoming perturbation at a node is commonly accepted in other systems—for example, in neuronal networks.

Throughout this article the length s of a shortcut is an important parameter that determines its dynamical and topological consequences for spatiotemporal chaos. s is defined as the minimum number of edges between the two end nodes of the shortcut, normalized by the number of nodes N in the network. For a network with even number of nodes the longest shortcut is $s=0.5$.

III. LIFETIME OF SPATIOTEMPORAL CHAOS IN THE PRESENCE OF A SINGLE SHORTCUT

The lifetime of spatiotemporal chaos on a regular ring network [5] is compared to the lifetime when a single shortcut of length s is added to the network. For each network realization the same 100 randomly chosen initial conditions for spatiotemporal chaos were used [41] and the shortcut was added after spatiotemporal chaos fully developed. Figure 1(a) shows a clear increase of the average lifetime T of spatiotemporal chaos with shortcut length s for small shortcuts

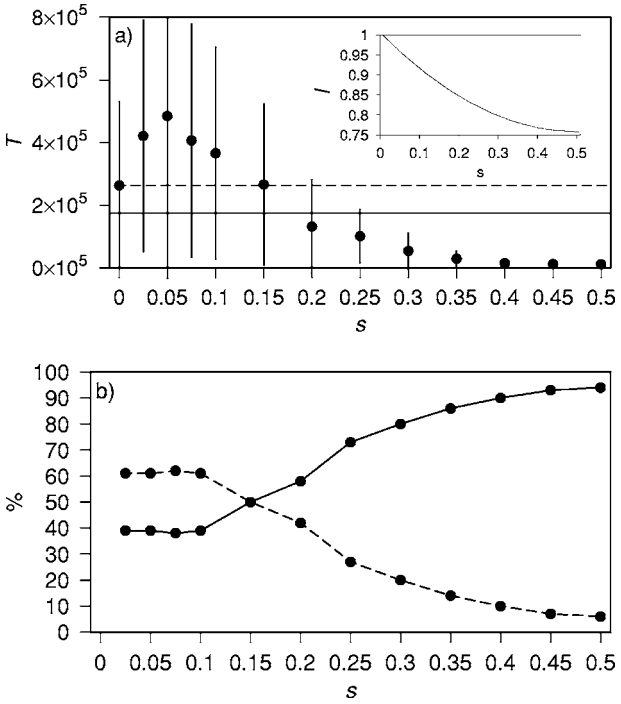

FIG. 1. (a) Average transient lifetime T of spatiotemporal chaos versus shortcut length s. The ring network consists of $N=180$ nodes with no shortcut ($s=0$, dashed horizontal line) and with a single added shortcut ($s>0$). Each data point was determined from 100 randomly chosen initial conditions for spatiotemporal chaos [41] and a fixed location for the shortcut of length s. The error bars were calculated as one standard deviation. Equation (1) was integrated with an explicit Euler method and a numerical time step $dt=0.0003$; the system parameters are $\mu=33.7$, $\Phi=2.8$, and $D=16$. The solid horizontal line represents the averaged transient time over all shortcuts of length $s>0$. The inset graph shows the analytically calculated characteristic path length l as a function of the shortcut length s, where l is normalized with the characteristic path length of the regular network ($s=0$). (b) Percentage of simulations from (a) in which the presence of a single shortcut decreased (solid line) or increased (dashed line) the transient time for the regular ring network ($s=0$) as a function of the shortcut length s.

$s\leqslant 0.05$. With further increase of the shortcut length, however, the lifetime T starts to decrease and falls below the value for the regular ring network at $s=0.15$. These two distinct regimes separated by $s=0.05$ point to two competing dynamical consequences of the shortcut, discussed below. For small shortcut length s the statistical fluctuations in the lifetimes of spatiotemporal chaos are large and comparable to the ones on the regular network ($s=0$). For larger shortcut lengths spatiotemporal chaos collapses rather quickly, which prevents large statistical fluctuations in T [42]. Figure 1(a) also demonstrates that the total average transient time over all shortcut lengths with $s>0$, an approximation of the lifetime for random single shortcuts, is reduced in comparison to the regular ring network.

In the regime $s\geqslant 0.05$ the decrease of the mean transient time with s for longer shortcuts is consistent with the decrease in the average characteristic path length l of the network [inset of Fig. 1(a)]. l is defined as the average shortest distance between any pairs of nodes in the network, normalized with the average shortest distance for the corresponding regular ring network. A shortcut that spans a few nodes changes the characteristic path length only a little, while the largest possible shortcut $s=0.5$, which spans half the nodes, yields the minimum average path length $l_{min}=(3N^2+6N-8)/4N^2$ [43]. For large networks $N\to\infty$, l_{min} approaches 0.75. It is frequently reported [20,34] that networks of size N with a smaller average path length exhibit a higher synchrony in their dynamics than those with larger l. Synchrony in the form of a quasihomogeneous network is an essential precursor to the collapse of spatiotemporal chaos on a regular ring network [Eqs. (1) and (2)]. In this quasihomogeneous state diffusive perturbations that normally initiate reaction-diffusion fronts and thus sustain spatiotemporal chaos are subthreshold. The trajectories throughout the medium closely follow the heteroclinic connection from the unstable focus to the stable node S^n, and the system reaches its stable, spatially homogeneous asymptotic state. The presence of a shortcut reduces the average path length in the network and promotes the quasihomogeneous medium to statistically advance the collapse of spatiotemporal chaos.

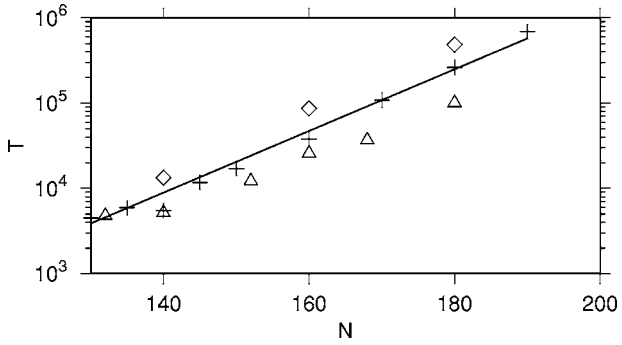

FIG. 2. Average lifetime T of spatiotemporal chaos versus number of nodes N for the ring network with no shortcut (+) and with a single shortcut of lengh $s=0.05$ (◇) and $s=0.25$ (△). The solid line shows a "robust least absolute deviation" fit of the average lifetimes for the regular ring network [5]. All of the other parameters are the same as in Fig. 1.

In the regime $s\leqslant 0.05$, however, the monotonic decrease of l with s is in contrast to the increase of the average lifetime T [Fig. 1(a)]. This points to another dynamical mechanism of the shortcut, which outweighs the effects of the decreasing l. This mechanism is further supported by Fig. 1(b), which shows that a shortcut of length s does not always decrease the lifetime of spatiotemporal chaos. Even for $s=0.5$, where the characteristic path length l is reduced by approximately 25%, some simulations show a delay in the collapse of spatiotemporal chaos. Insight into delay mechanisms for the collapse is given in the next section from a detailed local analysis of the dynamics at the shortcut nodes rather than from a global network parameter like l.

On a regular ring network the lifetime of spatiotemporal chaos increases exponentially with the network size N [5]. In the presence of a shortcut the exponential dependence persists as shown in Fig. 2 for two characteristic shortcut lengths. For a long shortcut ($s=0.25$ in Fig. 2) T increases slower than for the regular network, and for a small shortcut ($s=0.05$) the increase is stronger than for the regular case.

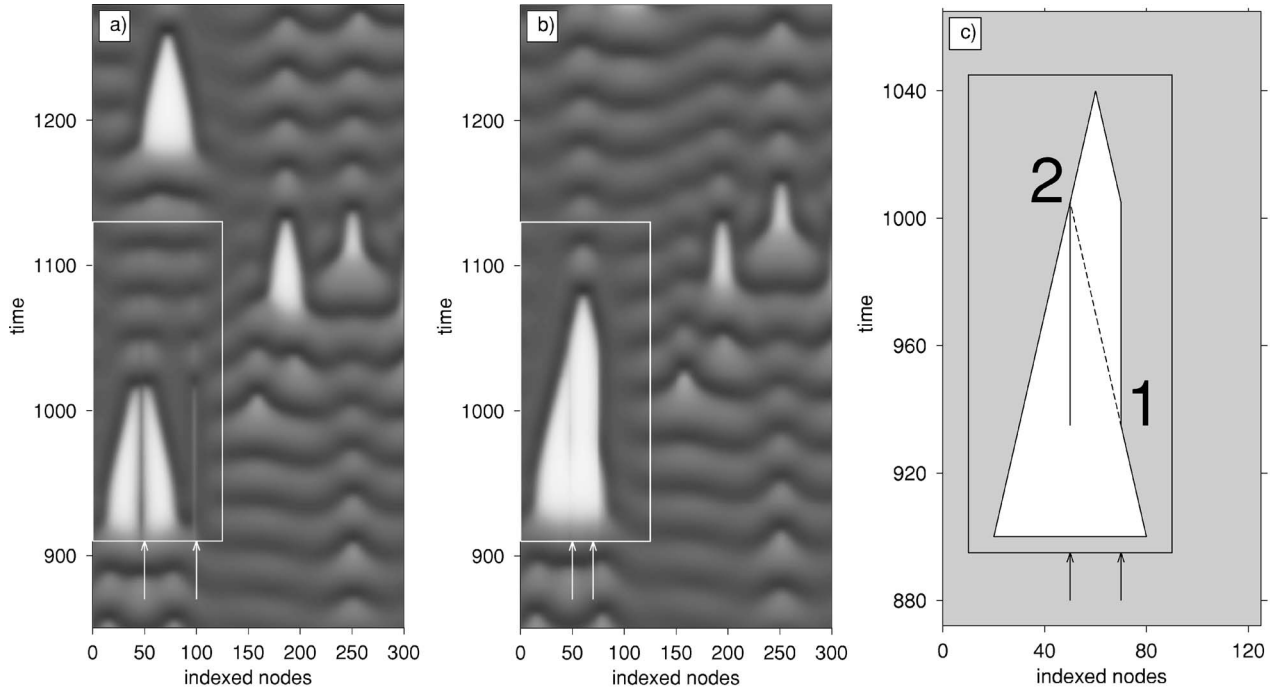

FIG. 3. Spatiotemporal dynamics of resource concentration a on a ring network ($N=400$, single shortcut) in the presence of an interface. The simulations in (a) and (b) differ by the length of the shortcut. In (a) the shortcut is made between node 50 and node 95 with a length of $s=0.11$, and in (b) the shortcut is made between node 50 and node 70 with a length of $s=0.05$. The box marks the presence of an interface in the neighborhood of the shortcut. The shortcut was added after spatiotemporal chaos developed. The initial conditions consist of a homogeneously distributed reactant A, $a=1$, over the entire network and randomly seeded species with concentration $b=1$ [5]. A reactant concentration of $a=1$ ($a=0$) is represented in white (black). All the other numerical and system parameters are the same as in Fig. 1. (c) outlines important features of a local extinction of type (b). The closed solid line marks the region of local extinction; an interface in the form of a vertical line forms at point (1) and deteriorates at the time corresponding to point (2). Such an interface is always accompanied by a second vertical line at the left end of the shortcut within the extinct region. The dashed line indicates how the local extinction would evolve from point (1) in the absence of the shortcut to form a triangular pattern. In (a)–(c) the arrows mark the left and right ends of the single added shortcut.

IV. LOCAL DYNAMICAL CONSEQUENCES OF A SINGLE SHORTCUT

Spatiotemporal chaos on a regular ring network is characterized by an irregular distribution of local extinct regions in space and time, in which species B is extinct ($b=0$) and resource A recovers to its maximum value ($a=1$). The triangular shape of the extinction patterns ([5], Fig. 3) is due to the propagation of species B into regions of high resource concentration A from both sides. In the presence of a single shortcut [Eq. (3)] the extinction patterns that include one of the shortcut's end nodes are altered in shape due to the formation of an interface. A systematic analysis of these emergent local extinctions [13], together with a manipulation of the location and length of the shortcut, reveals a few representative interface patterns that are marked by boxes in Figs. 3(a) and 3(b). Outside the box, the shortcut is not visibly evident in the spatiotemporal dynamics although preliminary statistical results point to more local extinctions in the presence of nonlocal coupling. An interface forms when one end of the shortcut is within a local extinct region, while the other is not. Then the magnitude of the gradient and hence of the coupling term between the two linked nodes, n and $n+m$ in Eq. (3), is largest.

The mechanisms of interface formation in Figs. 3(a) and 3(b) are similar. In Fig. 3(a) the right end of the shortcut is initially outside the local extinction. The reaction-diffusion fronts enter the extinct regime from both sides to form a triangular pattern. The interface, which is located at the right end of the shortcut, exists as long as one shortcut is within the extinction regime and the other is not. This interface is caused when the nonlocal coupling "transports" species B to the inside of the extinct regime which provides a subthreshold perturbation to the extinct state S^n that cannot initiate and support a propagating reaction-diffusion front from within the extinct regime. Concurrent with the transport of B to the inside is the drainage of resource A from inside, where $a=1$, to the outside, where a is clearly smaller [Fig. 3(a)]. If the shortcut in Fig. 3(a) would be extended to the right the same qualitative interface pattern would arise.

In Fig. 3(b) the mechanism for the interface is similar except that the shortcut is initially completely within the local extinct region. Consequently the gradient between the linked nodes n and $n+m$ is zero and Eq. (3) reduces to Eq. (2). A reaction-diffusion front is entering the extinct region from both sides until at the time of point "1" [Fig. 3(c)] the right front meets the right end of the shortcut. An interface forms [right vertical line in Fig. 3(c)], since the concentration gradient along the shortcut is no longer negligible [44]: the

left end node is within the extinct region and the right end is outside. As in the previous case [Fig. 3(a)] the interface is maintained by the drainage of species B from outside into the extinct region along the shortcut and vice versa for resource A. In contrast to the previous case the interface at the right end node is located at the boundary of the local extinction and prevents the right reaction-diffusion front from entering the locally extinct region, since the perturbations at the boundary are below the excitability threshold due to the drainage of B along the shortcut. The interface disappears when the propagating reaction-diffusion front from the left meets the left end of the shortcut at the time of point "2" [Fig. 3(c)] such that the dynamics at both end nodes is similar and the concentration gradients along the shortcut are negligible. Consequently, drainage of A and B along the shortcut is absent and both reaction-diffusion fronts provide superthreshold perturbations to the stable extinct state S^n to propagate symmetrically into the local extinction from both sides.

During the presence of the interface the propagation of one wave front is halted in cases like that of Figs. 3(b) and 3(c). Consequently the local extinction lasts for a longer time than in the absence of the shortcut [dashed line in Fig. 3(c)] and thus delays the collapse of spatiotemporal chaos on the global network, since the boundary of a local extinction provides a superthreshold perturbation to the network dynamics to sustain the propagation of reaction-diffusion fronts [5]. To prolong a local extinction a shortcut must be entirely contained by that extinction [as in Figs. 3(b) and 3(c)]. This, together with the fact that the frequency of local extinctions decreases exponentially with increasing size, makes the delay mechanism most important for shorter shortcuts. For longer shortcuts, however, the decrease in path length dominates to advance the collapse of spatiotemporal chaos. Figure 1(a) shows an increased lifetime of spatiotemporal chaos for small shortcut lengths s and a decreased lifetime for larger s.

The concentration profiles for species B at successive moments in time (Fig. 4) provide further insight into the evolution of the concentration gradient along the shortcut and its consequences for the formation and deterioration of the interface in Fig. 3(b). At time $t=940$, just prior to the interface formation, the shortcut between nodes 50 and 70 is completely within the local extinct region and the gradient between its nodes is close to zero. At time $t=960$ species B has reached the right end of the shortcut. The interface is marked by two cusps located at the end nodes with a non-negligible concentration gradient. For $t>960$ the propagation of species B into the extinct region is essentially halted until at $t=1000$ the propagating species from the left has reached the left end of the shortcut. The gradient along the shortcut is clearly reduced, and the interface ceases. With further increasing time B continues to symmetrically move into the extinct region from both sides as it would in the absence of the shortcut.

V. CAN TWO SHORTCUTS MAKE TRANSIENT CHAOS ASYMPTOTIC?

A single shortcut that is initially located within an extinct region temporarily prevents species propagation from one side [Fig. 3(b)] into this region. Two shortcuts, however, can form two interfaces that together prevent species invasion from both sides isolating the local extinct region for all times [13] as shown in Fig. 5. Since the presence of a local extinction prevents the global collapse of spatiotemporal chaos, an asymptotic local extinction (stripe) makes transient spa-

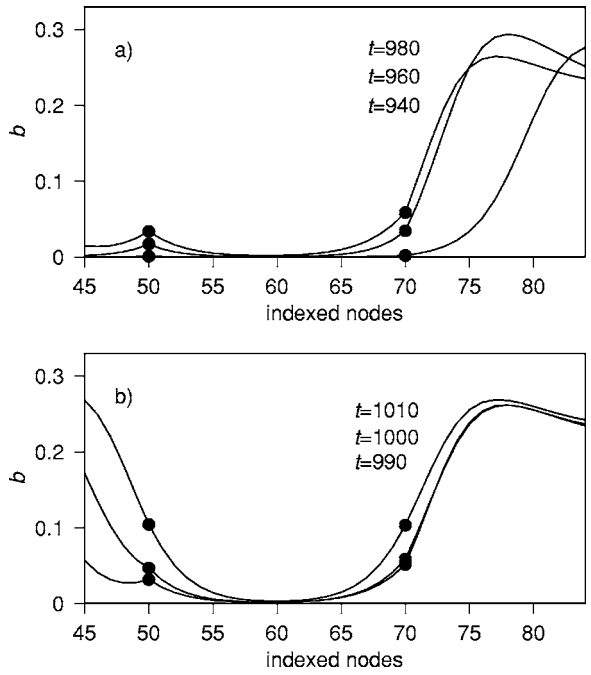

FIG. 4. Successive concentration profiles for species B during the formation (a) and deterioration (b) of the interface in Fig. 3(b). The shortcut between nodes 50 and 70 and all the other parameters are the same as in Fig. 3(b).

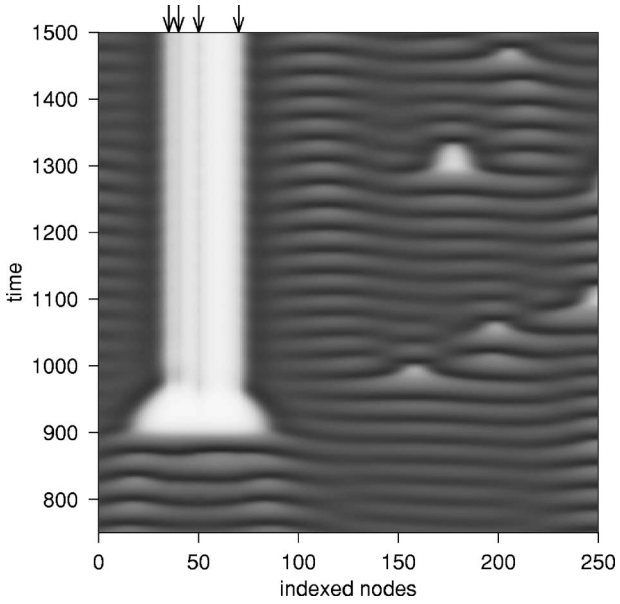

FIG. 5. Spatiotemporal dynamics of resource concentration a during stripe formation from two interfaces. Two shortcuts have been added to the ring network between nodes 30 and 45 and nodes 50 and 70 as marked. All the other numerical and system parameters are the same as in Fig. 3.

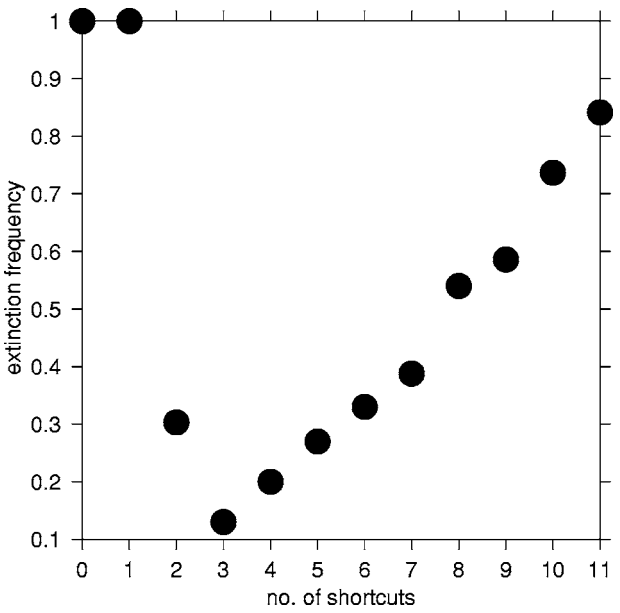

FIG. 6. Extinction frequency as a function of the number of added shortcuts in a ring network of $N=180$ nodes. Each data point corresponds to 100 simulations with randomly chosen shortcut locations and a fixed initial condition for spatiotemporal chaos. The extinction frequency describes the percentage of simulations in which spatiotemporal chaos collapsed before the formation of a stripe. All the other parameters are the same as in Fig. 1.

tiotemporal chaos asymptotic. Thus, only two shortcuts are necessary to prevent the collapse of spatiotemporal chaos in Eqs. (1) and (3) for any network size N, provided that the two (overlapping or nonoverlapping) shortcuts fall within a single local extinction to prevent species propagation from both sides. Adding two shortcuts can enhance synchrony in the local neighborhood by forming a stripe (Fig. 5), which in turn prevents synchrony of the entire network.

Two or more shortcuts, however, do not always prevent the collapse of spatiotemporal chaos since more shortcuts also cause a smaller average characteristic path length that promotes the collapse process as discussed in Sec. III. Spatiotemporal chaos on a ring network with nonlocal connections is governed by a competition between synchrony over the entire network and local synchrony. Synchrony over the entire network is expressed in the generation of an extinction of the size of the network to cause the transient behavior of spatiotemporal chaos. Local synchrony is expressed in the generation of local extinctions and stripes, with stripes causing asymptotic spatiotemporal chaos. In the presence of 2 shortcuts 27 out of 100 simulations (Fig. 6) show transient spatiotemporal chaos, whereas 73 simulations show asymptotic spatiotemporal chaos. This is in contrast to a ring network with no shortcut or with a single shortcut where all the simulations show transient chaos.

A preliminary statistical analysis of this competition between transient and asymptotic spatiotemporal chaos shows that transient chaos becomes less likely when increasing the number of shortcuts from 1 to 3 (Fig. 6). Such a decrease in global collapse frequency is consistent with the fact that an increasing number of shortcuts can provide a higher chance for stripe formation due to a higher chance of two simultaneous interface formations within a single local extinct region. If more than three shortcuts are added to the ring network, the chance for global extinction increases again with an increasing number of shortcuts, because the decreasing average path length dominates the synchronization properties in the network. We expect that this trend continues for an even larger number of shortcuts.

VI. CONCLUSIONS

Transient spatiotemporal chaos on a regular ring network of Gray-Scott excitable elements at each node becomes asymptotic with a chance of 70% with the addition of two shortcuts. This demonstrates that very small changes in the network's topology can profoundly alter the dynamics on the network. Even the addition of a single shortcut can drastically change the average lifetime of spatiotemporal chaos; short connections increase the average lifetime and long connections predominantly decrease it. The shortcut's dynamical consequence—i.e., the prevention of species propagation through interface formation—delays the global collapse of spatiotemporal chaos, while the shortcut's topological consequence—i.e., the reduction of the characteristic path length in the network—favors the collapse process. The latter is consistent with earlier studies where small-world topology improves synchronization in the network [19–21], since the collapse process in Eqs. (1) and (3) terminates in a globally synchronized state [5].

The master stability function [20,25] and its generalization for weighted networks [26] allows the quantification of the synchronization stability of linearly coupled dynamical elements. Further studies will explore the role of the master stability function for the collapse of spatiotemporal chaos on a regular ring network with and without added shortcuts. It will be of particular interest whether the local asymptotic synchronization pattern ("stripe"), which prevents the collapse of spatiotemporal chaos, is predicted by the master stability function, which is a quantity that describes the global network synchronization.

In some natural systems like ecological networks a dynamically changing network topology might be more realistic than the static topology considered in this article. The local synchronous pattern ("stripe") that prevents the collapse of spatiotemporal chaos in the static network will desintegrate if a shortcut is removed. Therefore, if the locations of added shortcuts change with time, spatiotemporal chaos will always be transient possibly with long transient times. The lifetime is determined by a competition between delay processes like the formation of local synchronous patterns ("temporary stripes") and interfaces, and processes that advance the collapse of spatiotemporal chaos like a shortcut-induced reduction of the average distance between any two nodes of the network.

Transient spatiotemporal chaos is also discussed as a source for species extinction in theoretical ecologies [9,10]. An increasing interest in spatiotemporal ecological dynamics [45] stems from the identification of spatial symmetry [46] as a possible cause of extinction, although the origin of spatial

synchronization is still under debate [47]. The Gray-Scott excitable dynamics in Eq. (1) phenomenologically mimics an ecological system, as it captures major ecological mechanisms like density-dependent species reproduction, competition for resource, a natural exponential species decay, and diffusion-based dispersal of species and resources. Long-distance movement like "hitchhiking insects in a truck" [48] are not accounted for by diffusive motion on a regular network but by the addition of nonlocal coupling in a network.

ACKNOWLEDGMENT

S.Y. thanks the University of Alaska Fairbanks for support.

[1] C. Grebogi, E. Ott, and J. A. Yorke, Physica D **7**, 181 (1983); T. Tel, in *Directions in Chaos III*, edited by H. Bai-lin (World Scientific, Singapore, 1990), pp. 149–211.
[2] G. Huber, P. Alstrom, and T. Bohr, Phys. Rev. Lett. **69**, 2380 (1992).
[3] A. Wacker, S. Bose, and E. Schöll, Europhys. Lett. **31**, 257 (1995).
[4] M. C. Strain and H. S. Greenside, Phys. Rev. Lett. **80**, 2306 (1998).
[5] R. Wackerbauer and K. Showalter, Phys. Rev. Lett. **91**, 174103 (2003).
[6] Y.-Ch. Lai and R. L. Winslow, Phys. Rev. Lett. **74**, 5208 (1995).
[7] J. P. Crutchfield and K. Kaneko, Phys. Rev. Lett. **60**, 2715 (1988).
[8] A. Politi, R. Livi, G. L. Oppo, and R. Kapral, Europhys. Lett. **22**, 571 (1993).
[9] K. McCann and P. Yodzis, Am. Nat. **144**, 873 (1994).
[10] L. Shulenburger, Y.-Ch. Lai, T. Yalcinkaya, and R. D. Holt, Phys. Lett. A **260**, 156 (1999).
[11] K. Kaneko, Phys. Lett. A **149**, 105 (1990).
[12] R. Wackerbauer and S. Kobayashi (unpublished).
[13] S. Rawoot, M.S. thesis, University of Alaska Fairbanks, 2004.
[14] D. J. Watts and S. H. Strogatz, Nature (London) **393**, 440 (1998); D. J. Watts, *Small worlds: The dynamics of networks between order and randomness* (Princeton University Press, Princeton, 1999).
[15] A.-L. Barabasi and R. Albert, Science **286**, 509 (1999).
[16] S. H. Strogatz, Nature (London) **410**, 268 (2001).
[17] E. Ravasz and A.-L. Barabasi, Phys. Rev. E **67**, 026112 (2003).
[18] V. M. Eguiluz, D. R. Chialvo, G. A. Cecchi, M. Baliki, and A. V. Apkarian, Phys. Rev. Lett. **94**, 018102 (2005).
[19] M. Kuperman and G. Abramson, Phys. Rev. Lett. **86**, 2909 (2001).
[20] M. Barahona and L. M. Pecora, Phys. Rev. Lett. **89**, 054101 (2002).
[21] X. F. Wang and G. Chen, Int. J. Bifurcation Chaos Appl. Sci. Eng. **12**, 187 (2002).
[22] H. Hong, M. Y. Choi, and B. J. Kim, Phys. Rev. E **65**, 026139 (2002).
[23] T. Nishikawa, A. E. Motter, Y.-Ch. Lai, and F. C. Hoppensteadt, Phys. Rev. Lett. **91**, 014101 (2003).
[24] A. E. Motter, C. Zhou, and J. Kurths, Phys. Rev. E **71**, 016116 (2005).
[25] L. M. Pecora and T. L. Carroll, Phys. Rev. Lett. **80**, 2109 (1998).
[26] M. Chavez, D.-U. Hwang, A. Amann, H. G. E. Hentschel, and S. Boccaletti, Phys. Rev. Lett. **94**, 218701 (2005).
[27] J. D. Noh and H. Rieger, Phys. Rev. Lett. **92**, 118701 (2004).
[28] P. G. Lind, J. A. C. Gallas, and H. J. Herrmann, Phys. Rev. E **70**, 056207 (2004).
[29] K. Iguchi and H. Yamada, Phys. Rev. E **71**, 037102 (2005).
[30] R. Pastor-Satorras and A. Vespignani, Phys. Rev. Lett. **86**, 3200 (2001).
[31] F. Qi, Z. Hou, and H. Xin, Phys. Rev. Lett. **91**, 064102 (2003).
[32] A. Zumdieck, M. Timme, T. Geisel, and F. Wolf, Phys. Rev. Lett. **93**, 244103 (2004).
[33] M. G. Cosenza and K. Tucci, Phys. Rev. E **65**, 036223 (2002).
[34] L. F. Lago-Fernandez, R. Huerta, F. Corbacho, and J. A. Siguenza, Phys. Rev. Lett. **84**, 2758 (2000).
[35] A. Roxin, H. Riecke, and S. A. Solla, Phys. Rev. Lett. **92**, 198101 (2004).
[36] D. He, G. Hu, M. Zhan, W. Ren, and Z. Gao, Phys. Rev. E **65**, 055204(R) (2002).
[37] P. Gray and S. K. Scott, Chem. Eng. Sci. **39**, 1087 (1984).
[38] J. H. Merkin, V. Petrov, S. K. Scott, and K. Showalter, Phys. Rev. Lett. **76**, 546 (1996); J. Chem. Soc., Faraday Trans. **92**, 2911 (1996); J. H. Merkin and M. A. Sadiq, IMA J. Appl. Math. **57**, 273 (1996).
[39] Y. Nishiura and D. Ueyama, Physica D **150**, 137 (2001).
[40] The weighted coupling coefficient $D_n=2D/k_n$ represents a special case of the weighing introduced in [24]. The network becomes directed due to the strengths of in-links and out-links of a node.
[41] An earlier study on the transient time of spatiotemporal chaos on regular networks with $N=120$ ($s=0$) showed that increasing the ensemble's size from 100 to 2000 only changed the mean transient time by 0.1% [5]. In the presence of a single shortcut, control calculations for $s=0.025$ ($s=0.2$) show that increasing the number of simulations from 100 to 140 (from 100 to 200) changes the average lifetime $\langle T\rangle$ by 6% (10%) only. These results confirm the qualitative relationship between transient time $\langle T\rangle$ and shortcut length s shown in Fig. 1(a).
[42] The frequency distributions of the transient lifetimes for $s=0$ [5] and for a control calculation with $s=0.2$ follow an exponential decay, which is consistent with the large absolute error bars in Fig. 1(a). For each shortcut length s, however, the error bars are of the order of the signal, having standard deviations above 80% of the average lifetime $\langle T\rangle$.
[43] The analytical expression of the normalized average path length l in the presence of a single shortcut with length s shows small differences for s even and s odd, which become negligible in the case of large networks $N\rightarrow\infty$. The formula in the text holds for s odd.
[44] The distance δ of the two trajectories at the end nodes, δ

$=\sqrt{(a_m-a_n)^2+(b_m-b_n)^2}$, is proportional to the magnitude of the gradient along the shortcut [13]. In the presence of the interface $\delta \approx 0.05$ is governed by a shortcut-induced shift of the stable steady state S^n, similar to the noise-induced shift of steady states in [49]. In the absence of the interface δ is clearly reduced.

[45] J. Bascompte and R. V. Sole, Trends Ecol. Evol. **10**, 361 (1995).

[46] M. Heino, V. Kaitala, and J. Lindstrom, Proc. R. Soc. London, Ser. B **264**, 481 (1997); D. J. D. Earn, P. Rohani, and B. T. Grenfell, *ibid.* **265**, 7 (1998).

[47] A. L. Lloyd and R. M. May, Tree **14**, 417 (1999); E. Ranta, V. Kaitala, and J. Lindstrom, Proc. R. Soc. London, Ser. B **266**, 1851 (1999); T. G. Benton, C. T. Lapsley, and A. P. Beckerman, Ecol. Lett. **4**, 1 (2001).

[48] R. S. Cantrell and C. Cosner, *Spatial Ecology via Reaction-Diffusion Equations*, Wiley Series in Mathematical and Computational Biology (Wiley, San Francisco, 2004).

[49] R. Wackerbauer, Phys. Rev. E **58**, 3036 (1998); **59**, 2872 (1999).